Available online at www.sciencedirect.com

ScienceDirect

Mendeleev Commun., 2020, **30**, 679–682

Mendeleev Communications

Electrochemical instability of bis(trifluoromethylsulfonyl)imide based ionic liquids as solvents in high voltage electrolytes for potassium ion batteries

Polina A. Morozova,*[a] Nikita D. Luchinin,[b] Dmitry P. Rupasov,[a] Natalia S. Katorova,[a] Stanislav S. Fedotov,[a] Victoria A. Nikitina,[a,b] Keith J. Stevenson[a] and Artem M. Abakumov[a]

[a] *Center for Energy Science and Technology, Skolkovo Institute of Science and Technology, 143025 Moscow, Russian Federation. E-mail: polina.morozova@skoltech.ru*

[b] *Department of Chemistry, M. V. Lomonosov Moscow State University, 119991 Moscow, Russian Federation*

DOI: 10.1016/j.mencom.2020.09.043

The feasibility of four ionic liquids containing bis(trifluoromethylsulfonyl)imide anion with different cations, namely 1-butyl-1-methylpyrrolidinium, 1-butyl-3-methylimidazolium, 1-methyl-1-propylpyrrolidinium and 1-ethyl-3-methylpyridinium, as solvents in an electrolyte of potassium ion batteries has been examined in half-cells with Al, Al_2O_3 as well as with practical cathode and anode materials. In spite of the previous reports on stability of ionic liquids with this anion in the 5 V limit, intrinsic electrochemical instability has been observed here both at high and low potentials, thus the investigated compounds can hardly be implemented in potassium ion cells due to their reactive nature.

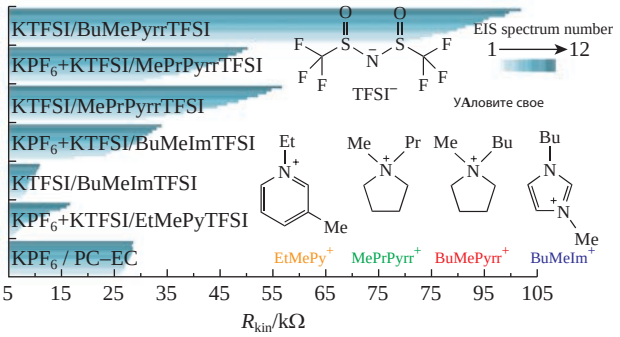

Keywords: potassium ion battery, high voltage, polyanionic cathode material, hard carbon anode, ionic liquids, high voltage electrolyte, electrolyte testing, bis(trifluoromethylsulfonyl)imide.

Potassium ion batteries (PIBs) represent an economically reasonable alternative to lithium ion batteries (LIBs) for large-scale energy storage due to potassium abundance in the Earth's crust and its availability. Within a common architecture, PIBs were shown to have large energy density values originated from the lower standard K^+/K potential in propylene carbonate-based solvents[1] and from use of high capacity cathode materials, such as Prussian Blue analogues with gravimetric energy density up to 510 W h kg^{-1} in half-cells,[2–4] layered oxides[5,6] and polyanionic compounds.[7,8] Particularly, $KVPO_4F$ represents a promising cathode material of 4 V class (*i.e.*, so called 'high voltage' range)[9–11] and a candidate for high power applications.

Since PIBs based on polyanionic cathode materials with high energy density generally operate at potentials exceeding 4.5 V *vs.* K^+/K,[10,12,13] at which carbonate derived electrolytes tend to decompose,[14–16] thermally stable electrolyte solutions are in demand. Aprotic ionic liquids (ILs) with wide electrochemical stability windows are typically used for electrolytes in LIBs[17,18] and sodium ion batteries[19] (SIBs) due to their advantages over conventional carbonate electrolytes, namely non-flammability as well as reasonable electrochemical and thermal stability.[20] For example, it is known that ILs based on bis(trifluoromethylsulfonyl)imide (TFSI) demonstrate both theoretical[21] and experimental[17,22–26] electrochemical stability at the 5 V limit required for high voltage operation.

To shed light on the ILs application for electrolytes in PIBs, in this work we have investigated electrochemical properties of IL interfaces with aluminum and α-alumina as well as with representative cathode and anode materials, namely $KVPO_4F$[10] and hard carbon,[27] respectively, in two electrode cells and report on here the electrochemical stability windows and interfacial resistance data for the selected electrolytes containing the KTFSI and KPF_6 salts.

Four commercially available ILs used in this work represented the salts of TFSI anion with the following cations: 1-butyl-3-methylimidazolium (BuMeIm), 1-methyl-1-propylpyrrolidinium (MePrPyrr), 1-butyl-1-methylpyrrolidinium (BuMePyrr) and 1-ethyl-3-methylpyridinium (EtMePy) (for details, see Online Supplementary Materials). All the explored ILs were previously reported to possess exceptional stability towards oxidation with the onset of oxidation at more than 4.5 V *vs.* Li^+/Li.[21,23,28–30]

At first, to examine the stability of aluminum current collectors in the electrolytes, we performed cyclic voltammetry (CV) measurements in ILs containing 0.5 M KTFSI [Figure 1(*a*)] and 0.1 M KTFSI + 0.111 M KPF_6 [Figure 1(*b*)] as well as compared their oxidative stability with that for the carbonate type electrolyte, namely 0.5 M KPF_6 in propylene carbonate–ethylene carbonate (PC–EC, 1 : 1 v/v), in two-electrode cells with potassium metal anode and aluminum current collector as a working electrode at 50 μV s^{-1}. The higher currents for the reverse (cathodic) scan compared with the forward (anodic) scan ones for the solutions containing KTFSI indicated a pronounced aluminum corrosion [see Figure 1(*a*)]. The known use of highly concentrated KTFSI solutions to achieve an efficient passivation of aluminum[31] was not feasible here due to the moderate solubility of KTFSI in the investigated ILs.

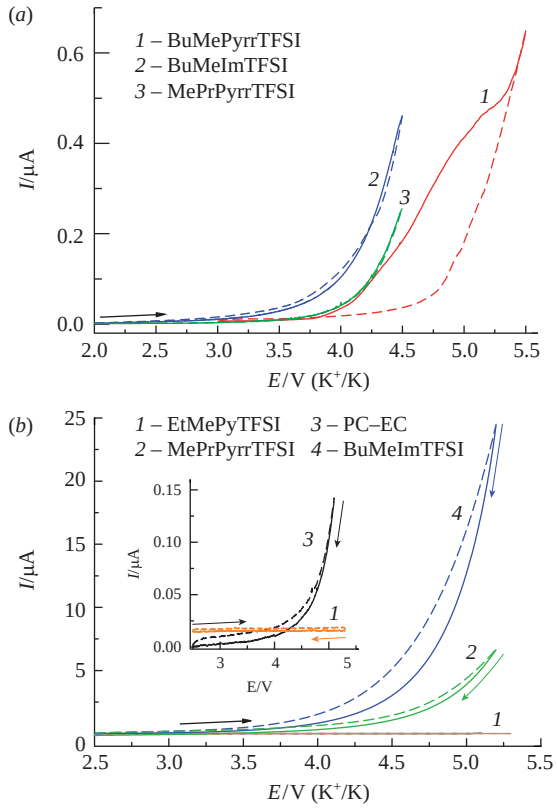

Figure 1 CV curves of Al working electrode (5th cycle at 50 μV s^{-1}) for (*a*) 0.5 M KTFSI in ILs as well as (*b*) 0.1 M KTFSI + 0.111 M KPF_6 in ILs and 0.5 M KPF_6 in PC–EC as electrolytes. Dashed line indicates forward scan, solid line indicates the reverse one. Inset represents enlarged CV curves for KPF_6 in PC–EC and KTFSI + KPF_6 in EtMePyTFSI.

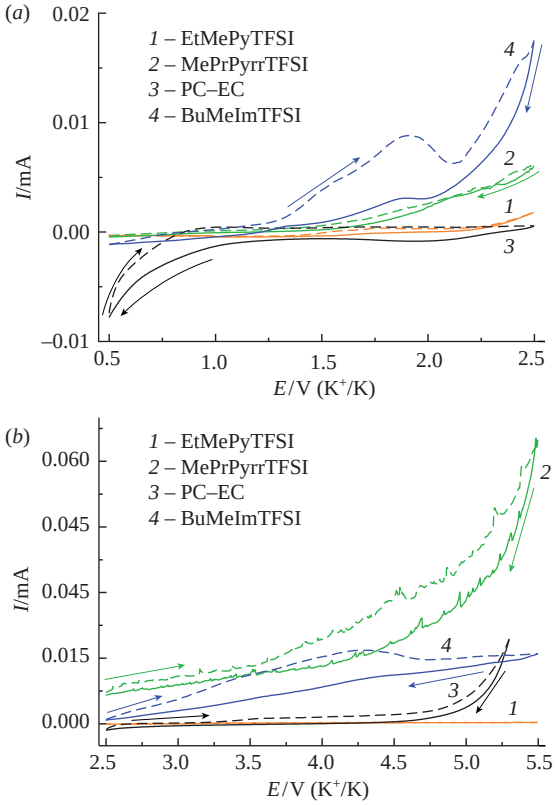

Figure 2 CV curves of Al_2O_3 working electrode (10th cycle at 50 μV s^{-1}) for (*a*) 0.5–2.5 as well as (*b*) 2.5–5.5 V potential ranges using 0.1 M KTFSI + + 0.111 M KPF_6 in ILs and 0.5 M KPF_6 in PC–EC as electrolytes. Dashed line indicates forward scan, solid line indicates the reverse one.

In contrast to the TFSI derived electrolytes, addition of KPF_6 clearly prevented the aluminum depassivation, as was evident from suppressed currents at the reverse scans in Figure 1(*b*), presumably due to formation of poorly soluble aluminum fluorides at the current collector surface. However, most IL-based electrolytes demonstrated much higher anodic currents than those observed in the PC–EC electrolyte [Figure 1(*b*), inset], except for EtMePyTFSI, which revealed extremely low currents even at the 5.0 V limit. The potentials of oxidation onset E_{ox} for 0.5 M KTFSI and 0.1 M KTFSI + 0.111 M KPF_6 solutions in ILs as well as 0.5 M solution of KPF_6 in PC–EC as electrolytes were determined at cut-off currents being 10 times higher than the background values. The E_{ox} values were 3.8 V for BuMeImTFSI, 4.3–4.5 V for MePrPyrrTFSI and BuMePyrrTFSI, while E_{ox} value for the KPF_6/PC–EC electrolyte was close to 5.0 V. Among all the ILs explored, EtMePyTFSI seemed to demonstrate an exceptional stability towards oxidation, its E_{ox} value at the fifth cycle could not be determined as the current values never exceeded the background value by 10 times. However, we noted that in this IL high oxidation currents were detected at the initial cycles (for details, see Online Supplementary Materials), which implied formation of cathode–electrolyte interfacial (CEI) layers rather than thermodynamic stability of EtMePyTFSI at high potentials.

Then, to consider more realistic working electrode morphology, we tested the electrolytes in two-electrode cells with composite alumina-based working electrode and potassium metal counter electrode. Employment of the composite electrode with electrochemically inactive material, namely 0.4 μm alumina powder layer with 10% carbon black and 10% poly(vinylidenefluoride) ensured the porosity and carbon content typical of practically used electrodes.[32] The 'idle' alumina working electrodes thus allowed capturing the electrolyte reduction/oxidation currents without the interference of intercalation ones, while inclusion of a carbon additive was important due to its reactive nature resulting in formation of solid–electrolyte interface (SEI) or CEI (see above).[33]

We also explored the cathodic potential range of 0.5–2.5 V [Figure 2(*a*)] and the anodic one of 2.5–5.5 V [Figure 2(*b*)] for 0.1 M KTFSI + 0.111 M KPF_6 in ILs as electrolytes with the alumina composite electrode. In the 0.5–2.5 V range the stabilized CVs for 10th cycles in BuMeImTFSI and MePrPyrrTFSI demonstrated relatively low reductive currents. However, notable oxidation waves appeared on the forward (anodic) scans [see Figure 2(*a*)], which were more pronounced for BuMeImTFSI. This indicates reoxidation of the electrolyte decomposition products reduced at the previous cathodic sweep and provides evidence for the absence of stable SEI formation at low potentials in the IL-based electrolytes. Since exceptionally high anodic currents were observed for BuMeImTFSI and MePrPyrrTFSI, these currents should correspond to the reoxidation of products formed at the potassium–ionic liquid interface and diffused towards the working electrode surface. Note that the cathodic current was generally higher in the PC–EC electrolyte [see Figure 2(*a*)], but no reoxidation events took place at the reverse scan, which indicated the appearance of a relatively stable SEI. Again, we suppose that the stability of EtMePyTFSI is only apparent, as during the initial cycles in the 0.5–2.5 V potential range, the observed anodic waves indicate reoxidation of the products formed during the reaction of potassium metal with the IL (for details, see Online Supplementary Materials). In the 2.5–5.5 V range, the stabilized CVs of composite alumina electrodes in EtMePyTFSI-containing electrolyte again showed no signs of electrochemical activity [see Figure 2(*b*)], which could indicate the formation of electronically insulating surface layers in this IL during the first cycles (for details, see Online Supplementary Materials). However, low currents after stabilization do not ensure the sufficient ionic conductivity of the interfaces formed, which will be further addressed in tests with practical electrode materials.

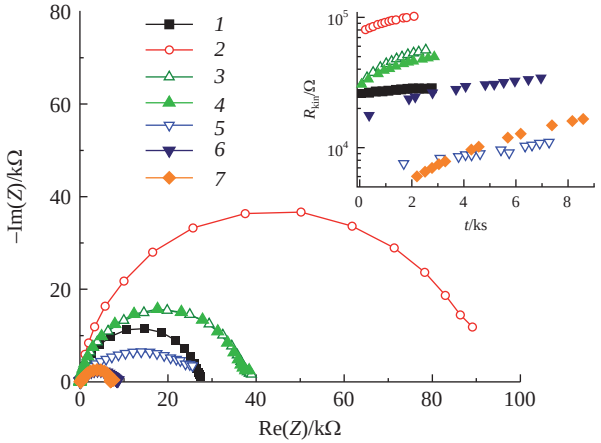

Figure 3 EIS spectra of K|electrolyte|K cells with IL and PC–EC electrolytes: (*1*) 0.5 M KPF_6 in PC–EC, (*2*) 0.5 M KTFSI in BuMePyrrTFSI, (*3*) 0.5 M KTFSI and (*4*) 0.1 M KTFSI/0.111 M KPF_6, both in MePrPyrrTFSI, (*5*) 0.5 M KTFSI and (*6*) 0.1 M KTFSI/0.111 M KPF_6, both in BuMeImTFSI, (*7*) 0.1 M KTFSI/0.111 M KPF_6 in EtMePyTFSI. Inset represents time evolution of the kinetic resistance R_{kin}.

To further understand and quantify the chemical interactions between potassium metal and the IL electrolytes, the electrolyte resistance R_{el} and surface layer kinetic resistance R_{kin} values were extracted from electrochemical impedance spectra (EIS) measured at open circuit voltage (OCV) at frequency range of 0.1 to 10 MHz and alternating voltage amplitude of 10 mV using two-electrode symmetric K|IL|K cells. The kinetic resistance values were calculated as diameters of the respective suppressed semicircles in the corresponding Nyquist plots (for details, see Online Supplementary Materials). The R_{kin} values were found to vary from 7 to 89 kΩ (Figure 3), which was by orders of magnitude higher than the SEI layer resistance for LIBs.[26] The impedance spectra at OCV were recorded continuously for 1–3 h, which allowed tracking an increase in the interfacial layers resistivity *vs.* time. The almost linear elevation of the R_{kin} values with time was observed for all the IL electrolytes, while the growth of the SEI resistance appeared to be the slowest for PC–EC one (Figure 3, inset). This result demonstrates that no SEI stabilization occurs in all the explored IL electrolytes. Note that although the EIS data suggests some stabilization of the potassium–(EC–PC) interface, the R_{kin} values are still exceedingly high, which would induce power limitations in a battery with potassium metal or other type of low-voltage anode.

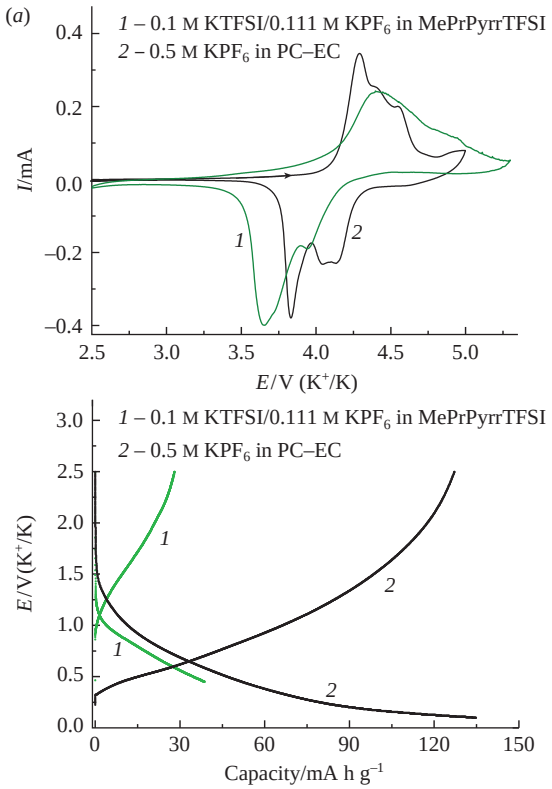

Figure 4 (*a*) CV curves of $KVPO_4F$ electrode (10^{th} cycle at 50 μV s^{-1}) and (*b*) charge–discharge profiles of hard carbon electrode at current density 30 mA g^{-1}, both for IL- and PC–EC-based electrolytes.

Electrochemical tests using $KVPO_4F$ as a practical PIB cathode and hard carbon anode in PC–EC and the ILs confirmed impossibility of IL-based electrolytes employment in PIBs. Indeed, CV data of $KVPO_4F$|K cells with MePrPyrrTFSI based electrolyte showed much higher peak-to-peak separations in ILs compared with PC–EC, which indicated an increased kinetic polarization in line with the EIS data [Figure 4(*a*)]. We note that the behavior of other ILs was even less stable compared with MePrPyrrTFSI due to the high reactivity of their components.

Voltammetric tests of $KVPO_4F$ half-cells using the EtMePyTFSI and BuMeImTFSI solutions demonstrated both remarkably low and stable currents after the first cycles in aluminum|IL or α-alumina|IL cells as well as relatively low R_{kin} values, and thus confirmed the assumption of the ionically insulating interface formation and electrochemical instability of these ILs. At the first three cycles in EtMePyTFSI and BuMeImTFSI, the oxidative currents dominated the electrochemical response of the $KVPO_4F$|K cell (for details, see Online Supplementary Materials), which indicated the intensive decomposition of the electrolyte, whereas after the fourth cycle the current dropped to near zero values, and no signs of reversible intercalation activity could be observed. This implies the ionically insulating nature of surface layers formed in these seemingly stable ILs. The lack of stabilization of the IL–anode interfaces also prevented reversible cycling of hard carbon anode in the MePrPyrrTFSI derived electrolyte, where the reversible capacity dropped from 140 to 40 mA h g^{-1} in PC–EC and the IL, respectively [Figure 4(*b*)].

Based on the reported results, we conclude that the intrinsic instability of the explored TFSI derived ILs limits their practical application in both high and low voltage domains, the poor low voltage stability being associated with the non-passivating SEI forming nature of the ILs, while the 5 V limit is inaccessible due to their insufficient oxidative stability.

S.S.F. and N.D.L acknowledge the support by the Russian Science Foundation (grant no. 18-73-00313). The authors are grateful to the Skolkovo Institute of Science and Technology (grant no. 2016-1/NGP).

Online Supplementary Materials

Supplementary data associated with this article can be found in the online version at doi: 10.1016/j.mencom.2020.09.043.

References

1 S. R. Basumallick and I. N. Basumallick, *J. Electrochem. Soc.*, 1990, **137**, 3876.
2 H. Kim, H. Ji, J. Wang and G. Ceder, *Trends Chem.*, 2019, **1**, 682.
3 L. Xue, Y. Li, H. Gao, W. Zhou, X. Lü, W. Kaveevivitchai, A. Manthiram and J. B. Goodenough, *J. Am. Chem. Soc.*, 2017, **139**, 2164.
4 A. Eftekhari, *J. Power Sources*, 2004, **126**, 221.
5 Y. Hironaka, K. Kubota and S. Komaba, *Chem. Commun.*, 2017, **53**, 3693.
6 H. Kim, D.-H. Seo, J. C. Kim, S.-H. Bo, L. Liu, T. Shi and G. Ceder, *Adv. Mater.*, 2017, **29**, 1702480.
7 N. Recham, G. Rousse, M. T. Sougrati, J.-N. Chotard, C. Frayret, S. Mariyappan, B. C. Melot, J.-C. Jumas and J.-M. Tarascon, *Chem. Mater.*, 2012, **24**, 4363.
8 C. Masquelier and L. Croguennec, *Chem. Rev.*, 2013, **113**, 6552.

9 K. Chihara, A. Katogi, K. Kubota and S. Komaba, *Chem. Commun.*, 2017, **53**, 5208.
10 S. S. Fedotov, N. R. Khasanova, A. Sh. Samarin, O. A. Drozhzhin, D. Batuk, O. M. Karakulina, J. Hadermann, A. M. Abakumov and E. V Antipov, *Chem. Mater.*, 2016, **28**, 411.
11 H. Kim, D.-H. Seo, M. Bianchini, R. J. Clément, H. Kim, J. C. Kim, Y. Tian, T. Shi, W.-S. Yoon and G. Ceder, *Adv. Energy Mater.*, 2018, **8**, 1801591.
12 V. A. Nikitina, S. M. Kuzovchikov, S. S. Fedotov, N. R. Khasanova, A. M. Abakumov and E. V Antipov, *Electrochim. Acta*, 2017, **258**, 814.
13 W. B. Park, S. C. Han, C. Park, S. U. Hong, U. Han, S. P. Singh, Y. H. Jung, D. Ahn, K.-S. Sohn and M. Pyo, *Adv. Energy Mater.*, 2018, **8**, 1703099.
14 B. B. Berkes, A. Jozwiuk, M. Vračar, H. Sommer, T. Brezesinski and J. Janek, *Anal. Chem.*, 2015, **87**, 5878.
15 B. Michalak, H. Sommer, D. Mannes, A. Kaestner, T. Brezesinski and J. Janek, *Sci. Rep.*, 2015, **5**, 15627.
16 M. Egashira, H. Takahashi, S. Okada and J.-i. Yamaki, *J. Power Sources*, 2001, **92**, 267.
17 A. Balducci, *Top. Curr. Chem.*, 2017, **375**, 20.
18 M. M. Huie, R. A. DiLeo, A. C. Marschilok, K. J. Takeuchi and E. S. Takeuchi, *ACS Appl. Mater. Interfaces*, 2015, **7**, 11724.
19 D. Monti, A. Ponrouch, M. R. Palacín and P. Johansson, *J. Power Sources*, 2016, **324**, 712.
20 A. P. Lewandowski, A. F. Hollenkamp, S. W. Donne and A. S. Best, *J. Power Sources*, 2010, **195**, 2029.
21 S. P. Ong, O. Andreussi, Y. Wu, N. Marzari and G. Ceder, *Chem. Mater.*, 2011, **23**, 2979.
22 M. P. S. Mousavi, B. E. Wilson, S. Kashefolgheta, E. L. Anderson, S. He, P. Bühlmann and A. Stein, *ACS Appl. Mater. Interfaces*, 2016, **8**, 3396.
23 T. Stettner, P. Huang, M. Goktas, P. Adelhelm and A. Balducci, *J. Chem. Phys.*, 2018, **148**, 193825.
24 V. R. Koch, L. A. Dominey, C. Nanjundiah and M. J. Ondrechen, *J. Electrochem. Soc.*, 1996, **143**, 798.
25 M. Galiński, A. Lewandowski and I. Stępniak, *Electrochim. Acta*, 2006, **51**, 5567.
26 A. Eftekhari, Y. Liu and P. Chen, *J. Power Sources*, 2016, **334**, 221.
27 Z. Jian, S. Hwang, Z. Li, A. S. Hernandez, X. Wang, Z. Xing, D. Su and X. Ji, *Adv. Funct. Mater.*, 2017, **27**, 1700324.
28 M. Hayyan, F. S. Mjalli, M. A. Hashim, I. M. AlNashef and T. X. Mei, *J. Ind. Eng. Chem.*, 2013, **19**, 106.
29 T. Yim, H. Y. Lee, H.-J. Kim, J. Mun, S. Kim, S. M. Oh and Y. G. Kim, *Bull. Korean Chem. Soc.*, 2007, **28**, 1567.
30 R. A. DiLeo, A. C. Marschilok, K. J. Takeuchi and E. S. Takeuchi, *J. Electrochem. Soc.*, 2013, **160**, A1399.
31 Y. Yamada and A. Yamada, *J. Electrochem. Soc.*, 2015, **162**, A2406.
32 O. A. Drozhzhin, V. A. Shevchenko, M. V. Zakharkin, P. I. Gamzyukov, L. V. Yashina, A. M. Abakumov, K. J. Stevenson and E. V. Antipov, *Electrochim. Acta*, 2018, **263**, 127.
33 P. M. Attia, S. Das, S. J. Harris, M. Z. Bazant and W. C. Chueh, *J. Electrochem. Soc.*, 2019, **166**, E97.

Received: 2nd March 2020; Com. 20/6147